*Accepted* NCHEM-12091229C

# Membrane-gated permeability in self-activated inorganic protocells

Mei Li,[1]* Rachel L. Harbron,[2] Jonathan V. M. Weaver,[2] Bernard P. Binks,[3] Stephen Mann[1]*

[1] Centre for Organized Matter Chemistry, School of Chemistry, University of Bristol, Bristol, BS8 1TS, UK
[2] Departments of Materials and Bioengineering, Imperial College London, London, SW2 7AZ, UK.
[3] Surfactant & Colloid Group, Department of Chemistry, University of Hull, Hull, HU6 7RX, UK.
*email: mei.li@bristol.ac.uk; s.mann@bristol.ac.uk

*Dedicated to the memory of J.V.M.W*

**Although several strategies are now available to produce functional micro-compartments analogous to primitive cell-like structures, little progress has been made in generating protocell constructs with self-controlled membrane permeability. Here we describe the preparation of water-dispersible silica nanoparticle-based colloidosomes that are delineated by a continuous, semi-permeable inorganic membrane capable of self-activated, electrostatically gated permeability. We use cross-linking and covalent grafting of a pH-responsive copolymer to generate an ultrathin, elastic membrane that exhibits selective release and uptake of small molecules. This behavior, which depends on the charge of the copolymer coronal layer, serves to trigger enzymatic dephosphorylation reactions specifically within the protocell aqueous interior. This system represents a step towards the design and construction of alternative types of artificial chemical cells and protocell models based on spontaneous processes of inorganic self-organization.**

Compartmentalization of primitive biochemical reactions within membrane-bound water microdroplets is a promising route to the organization and assembly of functional soft matter systems[1-3], and an essential step in elucidating the origin of life.[4,5] In general, attempts to model aspects of protocell construction and design have focused on the spontaneous self-assembly of enclosed organic membranes, usually in the form of lipid or fatty acid vesicles.[6-8] Whilst such an approach appears to offer the most plausible scenario for the origin of life, other models based for example on membrane-free peptide (polyelectrolyte)/nucleotide micro-droplets[9,10] or water-filled micro-compartments delineated by semi-permeable inorganic membranes,[11-13] are providing novel approaches to extending the technological scope for developing artificial chemical cells. In particular, the preparation of microscale compartments in the form of Pickering emulsions, which consist of a suspension of colloidal or nanoparticle-stabilized water micro-droplets (colloidosomes) in oil,[14] offers an important step towards the

construction of inorganic protocells that are capable of functioning as confined reaction environments for *in situ* gene expression[11] and enzyme-mediated catalysis.[11,15] These biomimetic properties have so far only been demonstrated in a continuous oil medium because transfer of the colloidosomes into bulk water induces disassembly of the closely packed nanoparticle-containing inorganic membrane and release of the entrapped biomolecular components. Thus, developing procedures that stabilize the inorganic membrane without compromising the level of semi-permeability required for the simultaneous retention of biomacromolecules and uptake/release of small molecule substrates is an important step towards the construction of water-dispersible inorganic protocells. However, even if it was possible to disperse intact colloidosomes in bulk water, their functionality and use as biomimetic protocells would be seriously undermined by passive diffusion of entrapped low molecular weight substrates through the semi-permeable membrane. As a consequence, mechanisms of restricted transport across the inorganic membrane need to be developed to prevent rapid discharge of the artificial cells at water/water interfaces. In this paper, we address these challenges by designing and constructing membrane-gated colloidosomes that can be transferred from oil into bulk water in the form of intact micro-capsules comprising a copolymer-grafted inorganic membrane with self-activated, electrostatically mediated permeability. We demonstrate how pH-responsive changes in copolymer charge at the surface of the inorganic membrane can be used to produce intact water-dispersible colloidosomes that exhibit selective permeability for anionic or cationic solutes, and exploit this mechanism for the construction of inorganic protocells with membrane-gated enzymatic activity.

Previous studies on colloidosome formation have demonstrated that the permeability, mechanical robustness and responsiveness of the micro-capsules are strongly dependent on the type and size of the constituent particles, post-assembly processing, and physical state of the interior,[14,16-18] and that transfer into an aqueous phase requires mechanical stabilization of the membrane by sintering or chemical cross-linking.[14,19-21] Tunable permeability can be engineered into the colloidosome organic shell by assembling the membrane from polymer microgel particles that exhibit temperature-dependent swelling/deswelling behaviour,[18] or by using an analogous polymer but as a scaffold for particle assembly such that temperature-dependent buckling of the internalized gel generates reversible jamming and buckling of the organic membrane.[22] In contrast, although inorganic nanoparticle-based colloidosomes have

been rendered impermeable by physical entrapment of poly-(D,L-lactic acid) within the interstitial void spaces of the membrane during sample preparation,[23] to the best of our knowledge, the construction of inorganic colloidosomes with membrane-responsive permeability has not been achieved. Herein, we demonstrate a strategy for achieving this goal (Fig. 1). In brief, a Pickering emulsion consisting of aqueous micro-droplets stabilized with a semi-permeable membrane of closely packed 20-30 nm-sized silica nanoparticles was initially prepared in dodecane. The membrane was subsequently cross-linked in oil by reaction with tetramethoxysilane (TMOS) to stabilize the inorganic matrix and facilitate phase transfer of intact colloidosomes into water. A pH-responsive copolymer was covalently grafted to the cross-linked inorganic membrane prior to phase transfer to provide an outer coronal layer capable of electrostatically mediating the diffusion of small molecules through the interstitial nanospaces of the silica nanoparticle-based shell. This was achieved by synthesizing a novel inorganic-organic copolymer **1**, with approximate composition, $TMSPMA_{23}/DMAEMA_{40}/MAA_{37}$-$EGDMA_8$-$DDT_{10}$ that was designed with a branched architecture of 3-(trimethoxysilyl)propyl methacrylate (TMSPMA), 2-(dimethylamino)ethyl methacrylate (DMAEMA), methacrylic acid (MAA), ethylene glycol dimethacrylate (EGDMA) and 1-dodecanethiol (DDT) moieties (Supplementary information and Fig. S1).

**Results and discussion**

The synthesis of copolymer **1** was based on previous methods used to prepare this class of branched, multi-functional copolymers.[24,25] Zeta potential measurements for an aqueous solution of **1** gave values of +20 and -30 mV at pHs of 2 and 10, respectively, with an isoelectric point at pH ≈ 5 (Supplementary Fig. S2a). This was consistent with pH titration curves of **1** that showed complex behaviour with an apparent $pK_a$ value of 5.76 (Supplementary Fig. S2b). Dynamic light scattering (DLS) studies showed the presence of discrete macromolecules at pH 2 and above pH 7, which were 30-40 nm in hydrodynamic diameter; in contrast, micrometer-sized aggregates were observed between pH values of 4 and 6, consistent with the low surface charge on the copolymer under these conditions (Supplementary Fig 2c).

We exploited the above properties and multi-functional nature of **1** to generate covalent linkages between the TMSPMA side chains and Si-OH groups on the exposed

surface of the colloidosome, and to provide a localized mechanism for modulating the electrostatically induced transfer of charged small-molecule aqueous solutes through the inorganic membrane. In the latter case, we used the pH-induced protonation/deprotonation of the copolymer carboxylic acid (MAA) and amino (DMAEMA) groups to induce reversible changes in ionic charge at the surface of the silica nanoparticle-based shell. As confirmed by the zeta potential measurements, protonation of both DMAEMA (pKa ≈ 10) and MAA side chains (pKa ≈ 4-4.5) produced a substantial positive charge on the copolymer at pH values between 2 and 4, whilst the branched macromolecule exhibited a considerable negative charge at pH 9 and above.

Addition of a dry powder of surface-active silica nanoparticles to a water-dodecane mixture at an aqueous volume fraction of 0.033 produced a suspension of well-defined, spherical micro-compartments up to 200 μm in mean diameter (Fig. 2a). While stable in the continuous oil phase, transfer of the micro-compartments into water by gradually changing the polarity of the continuous phase was unsuccessful due to disassembly of the closely packed nanoparticle membrane. In contrast, cross-linking of the inorganic shell with TMOS, or using a combination of cross-linking and covalent grafting of pH-responsive copolymer **1**, produced spherical colloidosomes that were transferred into the bulk water phase without loss of structural integrity (Fig. 2b, c). No transfer into water was observed for the polymer-grafted colloidosomes prepared without TMOS cross-linking. A considerable roughening in the surface texture of the inorganic membrane was observed after modification with TMOS (Supplementary Fig. S3) or TMOS/copolymer **1** (Fig. 2b). This was consistent with the presence of a cross-linked matrix of silica on the surface of the colloidosomes and slight shrinkage of the water drops during modification to produce a corrugated membrane surface. FTIR spectra of the transferred TMOS cross-linked colloidosomes showed strong Si-O-Si adsorption bands at around 470 and 1100 $cm^{-1}$, and CH vibrations at 807 $cm^{-1}$ and 2853-2927 $cm^{-1}$ attributed to Si-$CH_3$ groups on the surface of the nanoparticles (Supplementary Fig. S4). In addition to the silica vibration bands, the spectra of the cross-linked copolymer-grafted colloidosomes showed C-H deformation vibrations at 1380 and 1466 $cm^{-1}$ from N-$CH_3$ and N-$CH_2$, or N-$CH_3$ groups, respectively, a low intensity C=O stretching vibration at 1730 $cm^{-1}$, and high intensity C-H bands at 2853-2927 $cm^{-1}$, confirming the presence of the copolymer in the cross-linked colloidosomes after transfer into the continuous water phase. The

spectroscopic data were also consistent with C and H analyses on the water-transferred colloidosomes that showed an increase in the C and H contents from 9.86 and 2.28%, respectively, in the TMOS cross-linked micro-compartments to values of 10.37 and 2.31% in the cross-linked, copolymer-grafted functionalized colloidosomes.

We observed that the cross-linked, copolymer-functionalized micro-compartments did not collapse on air drying, but instead contracted into intact microspheres that were approximately half of the size of the initial colloidosome, and which exhibited an extensively wrinkled outer surface (Fig. 2d-f). Re-hydration of the dried colloidosomes restored their initial size, indicating that the nanoporous silica/copolymer membrane was structurally intact and mechanically elastic even in the dried state. A similar phenomenon was observed for TMOS cross-linked colloidosomes prepared without the grafted copolymer shell, indicating that the elastic behavior was associated specifically with the structure of the interconnected inorganic nanoparticle array.

Anionic (calcein, pKa values 2.1, 2.9, 4.2, 5.5, 10.8, 11.7), and cationic (acriflavine hydrochloride, rhodamine 6G ($pK_a$ = 7.5)) water-soluble fluorescent dye molecules (Supplementary Fig S5) could be readily encapsulated at pH 7 within the colloidosomes during self-assembly of the nanoparticle membrane in the oil phase. In each case, fluorescence microscopy images of the dye-containing colloidosomes dispersed in dodecane showed strong fluorescence intensities associated with the nanoparticle-stabilized micro-compartments (Fig. 3a, Supplementary Fig S6). Corresponding images of colloidosomes at internal pH values between 2 and 10 also displayed high fluorescence intensities (Supplementary Fig S7), even though calcein and to a lesser extent acriflavine hydrochloride showed pH-dependent fluorescence behaviour in bulk aqueous control solutions (Supplementary Fig. S8). Transfer of the cross-linked colloidosomes into water resulted in release of the dye molecules into the continuous phase independent of the pH of the external solution (Fig. 3b-d and Supplementary Fig S6), indicating that the nanoparticle membrane remained permeable to small molecules after pre-treatment with TMOS alone. In contrast, fluorescence images of cross-linked, copolymer-functionalized colloidosomes containing calcein, acriflavine hydrochloride or rhodamine 6G indicated that the dye molecules were retained within the colloidosome interior after transfer into water depending on the pH of the bulk solution (Fig. 3e-l) and Supplementary Fig. S9). The anionic and cationic dyes were retained to a considerable extent

at neutral pH, but released under acidic or alkaline conditions, respectively. Similar experiments with cross-linked, copolymer-functionalized colloidosomes containing encapsulated positively or negatively charged proteins such as cytochrome *c* or ferritin and myoglobin, respectively, showed no leakage across a pH range of 2-10 (Supplementary Fig. S10), indicating that the gating mechanism operated specifically at the molecular level.

UV spectroscopy was used to determine the release profiles for calcein or rhodamine 6G trapped within the cross-linked, copolymer-functionalized colloidosomes and exposed to bulk aqueous solutions at various pH values (Fig. 3m,n). The plots indicated that approximately 80% of the encapsulated calcein was released at pH 4 after 1 hr with a threshold level for the released dye attained within 2 hours of immersion (Supplementary Fig. S11). In contrast, entrapped rhodamine 6G was completely released at pH 9 although the kinetics appeared to be slower (80 and 100% after 4 and 8 hrs, respectively) compared with calcein transfer through the copolymer-functionalized inorganic membrane. Essentially no release was observed at pH values of 10 or 7 for calcein-containing colloidosomes, whilst rhodamine 6G was completely retained at pH 2 and exhibited a slow rate of leaching at neutral pH. These results were attributed to changes in the net charge of the copolymer-grafted layer from positive to negative as the pH was increased above the copolymer isoelectric point (pH = 5) and apparent $pK_a$ value of 5.76. As a consequence, increased electrostatic repulsion between the copolymer coronal layer and negatively charged calcein molecules or cationic acriflavine hydrochloride/rhodamine 6G molecules under alkaline (pH = 10) or acidic ($pH \leq 4$) conditions, respectively, provided an effective gating mechanism for the complete retention of the dye molecules within the colloidosome interior. At intermediate pH values, the multivalent nature of the polymer coronal layer appeared to be sufficiently charged at a local level to curtail the diffusion of cationic and anionic small molecules across the nanoparticle membrane, particularly in the case of calcein, which at neutral pH has a high spatial charge density associated with four negatively charged carboxylates and two positively charged amino groups.

Given these pH-induced changes in membrane permeability, we tested the ability of the cross-linked, copolymer functionalized colloidosomes to selectively inhibit the uptake of small molecules from the external solution. Incubation of non-dye-filled colloidosomes in aqueous solutions of buffered calcein at different pH values indicated that the micro-compartment membrane was impermeable to the anionic dye at pH 10, weakly permeable at

pH 7, and permeable at pH 4 (Fig. 4a-c), consistent with the release experiments. Similar experiments undertaken with water-filled colloidosomes dispersed in aqueous solutions of buffered acriflavine hydrochloride showed converse pH-dependent behavior with uptake of the cationic dye specifically inhibited at pH 2 (Fig. 4d-f). In contrast, pH-independent uptake was observed for cross-linked colloidosomes prepared in the absence of the grafted copolymer (Supplementary Fig S12). These data confirmed that pH-responsive transfer of charged molecules across the cross-linked, copolymer-functionalized inorganic membrane in either direction was strongly dependent on electrostatically mediated diffusion.

The above results indicated that water-dispersible colloidosomes with pH-dependent uptake and release properties can be prepared by cross-linking and copolymer modification of surface-active silica nanoparticles pre-organized at water/oil micro-droplet interfaces. These processes result in the formation of discrete microscale reaction environments that are enclosed within a continuous inorganic membrane, which is ultrathin, nanoporous, structurally robust and elastic, and exhibits self-activated electrostatically mediated permeability in response to changes in pH. As such, these microstructures could provide new opportunities for constructing alternative types of artificial chemical cells. As a step towards this goal, we carried out an enzyme-catalyzed reaction inside the water-in-water colloidosomes that was regulated by the gated properties of the inorganic membrane. Alkaline phosphatase (ALP) was encapsulated within the precursor water-in-oil Pickering emulsion at a constant concentration, and after cross-linking and copolymer modification of the silica nanoparticle shell, the bioinorganic protocell was transferred into water. A small-molecule anionic substrate, 4-nitrophenyl phosphate (*p*NPP, ($pK_a$ = 5.2, 5.8) was added at a constant concentration to the continuous aqueous phase maintained at various pH values, and the kinetics of formation of the enzymatically produced product, 4-nitrophenolate ($pK_a$ = 7.2), was determined by monitoring the absorption intensity of the continuous phase at 410 nm over time at 37 °C. The reaction rate of ALP-mediated dephosphorylation at pH of 8.4 was 0.42 μM/min, and increased to 0.75 μM/min when the pH increased to 9.1 (Fig. 5a), indicating that the inorganic protocells had considerable enzymatic activity. Thus, uptake of *p*NPP and release of 4-nitrophenolate into the continuous water phase readily occurred under these conditions. In contrast, increasing the pH to 9.8 gave a dramatic decrease in the reaction rate to 0.14 μM/min (Fig. 5a), which was suggestive of copolymer-mediated restricted transfer across the inorganic

membrane. This mechanism was consistent with results obtained by monitoring the ALP-mediated reaction under the same enzyme and substrate concentrations but within cross-linked colloidosomes prepared without the copolymer corona and dispersed in water, which showed no pH-mediated inhibition at pH 9.8 (Fig. 5b). Instead, the reaction rates increased progressively from 0.41 to 0.79 to 1.02 μM/min at pHs of 8.4, 9.1 and 9.8, respectively. These values showed the same trend as for control reactions performed at the same pH values and under the same concentrations in bulk aqueous solution in the absence or presence of copolymer-functionalized silica nanoparticles except that the bulk phase reaction rates were considerably increased (12.2, 18.4 and 22.3 μM/min or 14.5, 19.6 and 23.6 μM/min, respectively) and the time for the reaction to come to completion considerably decreased from several hours to a few minutes (Fig. 5c, Supplementary Fig. S13).

The absence of a yellow colouration within the colloidosome dispersion indicated that the change in enzyme kinetics observed at pH 9.8 was not associated with formation and entrapment of 4-nitrophenolate within the micro-compartments but attributed to the inhibition in the transfer of the di-anionic *p*NPP substrate into the cross-linked copolymer-functionalized colloidosomes due to the high negative charge on the inorganic membrane. As a consequence, the enzyme reaction was essentially switched off, but could be restored by reducing the electrostatic repulsion between the substrate and grafted copolymer corona by decreasing the pH (Fig. 5d). In contrast, the initial rate of dephosphorylation within colloidosomes prepared without the copolymer corona remained substantial at pH 9.8, consistent with the presence of a passive semi-permeable inorganic membrane. The fact that the rates were so much faster in bulk solution compared with the colloidosomes suggested that the nanoscale porosity of the cross-linked silica nanoparticle membrane acted as a considerable diffusional barrier even in the absence of the pH-gated copolymer coronal layer. However, we cannot rule out the possibility that the presence of sterically hindered or denatured active sites associated with adsorption of the encapsulated proteins onto the silica nanoparticle surfaces was responsible for the differences in enzyme kinetics.

## Conclusions

The first steps towards the chemical construction of an enzymatically active bio-inorganic protocell with self-mediated, electrostatically gated permeability at water-water phase

boundaries have been demonstrated by copolymer modification of the outer surface of a cross-linked, enveloped membrane of closely packed silica nanoparticles. Covalent grafting of the pH-responsive copolymer is facile, suggesting that additional modifications in the properties of the hybrid membrane could be tuned by judicious chemical and structural design of the multi-charged, extensively branched macromolecules. Moreover, the intrinsic elasticity of the hybrid membrane provides a robust micro-architecture that can withstand dehydration and re-hydration without loss of membrane functionality, suggesting that it should be possible to exploit the functionalized colloidosomes in applications involving the long term storage of biomacromolecules, recursive uptake of substrates and cofactors, or sustained self-controlled release of drug and bioactive agents. In this regard, the cross-linked copolymer-functionalized colloidosomes dispersed in oil or water were stable at high temperatures for considerable periods of time (e.g. 80°C, 4 hours; see Supplementary Fig. S14) suggesting that they could be exploited under adverse conditions, as well as for applications involving temperature cycling procedures such as in the amplification of entrapped genetic material by polymerase chain reaction methods. Finally, our results open up new horizons in protocell research, providing novel opportunities for advancing the design and construction of inorganic cell-like constructs that are energized via membrane-mediated chemical potential gradients, and which therefore could sustain compartmentalized processes under non-equilibrium reaction conditions. Such systems might also provide an alternative model of abiogenic self-organization that offers useful insights into current theories on the geochemical origin of proto-metabolic cycles on the early Earth.[26]

## Methods

**Materials.** Partially hydrophobic silica nanoparticles with spherical morphology and primary mean diameter of 20–30 nm were prepared as described previously.[11, 27] In brief, hydrophilic silica nanoparticles were silylated to various extents by reaction with dichlorodimethylsilane in the presence of water followed by drying at 300°C for 2 h. The particular particles used here were surface-functionalized with *ca.* 50% silanol (–$O_3SiOH$) and 50% dimethylsilane (–$O_2Si(CH_3)_2$) groups. Partially hydrophobic clay sheets (200-1000 nm in width) were prepared from synthetic hectorite that was partially coated with a di-hydrogenated tallow dimethylammonium salt (Laponite, Rockwood Additives Ltd, OML, OG (SR 4232)). Calcein (bis[*N*,*N*-bis(carboxymethyl)aminomethyl]fluorescein, $C_{30}H_{26}N_2O_{13}$, $\lambda_{ex}$ = 470 nm; $\lambda_{em}$ = 509 nm), acriflavine hydrochloride (3,6-diamino-10-methylacridinium chloride hydrochloride, Euflavine, $C_{27}H_{28}Cl_4N_6$, $\lambda_{ex}$ = 416 nm; $\lambda_{em}$ = 514 nm), glycine, alkaline phosphatase (ALP, 1000U/mg), phosphatase substrate (4-nitrophenyl phosphate (*p*NPP), disodium salt hexahydrate), anhydrous dodecane, 3-(trimethoxysilyl)propyl methacrylate (TMSPMA), 2-(dimethylamino)ethyl methacrylate (DMAEMA), methacrylic acid (MAA), ethylene glycol dimethacrylate (EGDMA), 1-dodedanethiol (DDT), and anhydrous methanol were purchased from Sigma-Aldrich, and used as received. Tetramethoxysilane (TMOS) was purchased from Fluka, UK. Azobis(isobutyronitrile) (AIBN) was purchased from BDH and recrystallized from methanol prior to use.

**Preparation and characterization of pH-responsive copolymer.** TMSPMA, DMAEMA, MAA, branching monomer (EGDMA), dodecanethiol and anhydrous methanol were added to a glass vessel equipped with a stirrer bar in pre-determined molar ratios and degassed by nitrogen purge for 30 mins. The solution was heated to 70 ºC under an inert atmosphere. Polymerization was started by addition of AIBN and the reaction was left stirring for 48 h. After this time monomer conversions in excess of 97 % were typically achieved and dry methanol was removed by evaporation at reduced pressure. No purification steps were required due to almost complete conversion. The resulting materials were stored in dry methanol under nitrogen and then characterized.

Molecular weights, molecular weight distributions and Mark-Houwink α-values were measured in THF using a triple detection gel permeation chromatography (TD-GPC) system. The THF system used was a Viscotek TDA-302 TD-GPC equipped with two ViscoGel HHR-N columns and a guard column with a mobile phase of THF and triethylamine (2.5 %) at 35 ºC and a flow rate of 1 mL $min^{-1}$. Samples for NMR spectroscopy were recorded in $CDCl_3$ using a Bruker 400 Ultrashield spectrometer operating at 400 MHz.

Hydrodynamic copolymer size distributions and zeta potential values were measured by dynamic light scattering (DLS) using a Malvern Zetasizer (Nano series) Nano-ZS equipped with a 633 nm laser. The scattering angle used was 175°, and all samples were measured in a disposable polystyrene cuvette. In general, 1 mL of the dilute copolymer solution was added

to the dispersion unit at pH values of 10, 9, 7, 5, 4, and 2. The volume-average diameters and zeta potential values were obtained from at least 3 repeated runs.

The pKa of the copolymer was determined by monitoring the change in pH of a copolymer solution initially at pH 10 after addition of 0.025 mL increments of 0.1M hydrochloric acid to a final pH value of 2. The pKa was determined from an average of 3 repeat runs.

FTIR spectroscopy (Perkin-Elmer Spectrum I; KBr disks) was undertaken on air-dried TMOS-cross-linked colloidosomes or TMOS-cross-linked, copolymer functionalized colloidosomes. The samples were prepared as described above and investigated after transfer into a continuous water phase. Spectra were also recorded on samples of copolymer **1** after air drying from methanol solutions.

**Preparation of water-dispersed copolymer-gated colloidosomes**. Nanoparticle-stabilized water-in-oil emulsions were prepared based on previous methods.[11] Typically, 20 mg of partially hydrophobic silica nanoparticles were mixed with or without 1 mg of partially hydrophobic clay particles (the presence of the clay had no influence on the reported results), and 3 mL of anhydrous dodecane was then added. The resultant mixture was sonicated in an ultrasound bath for 20 seconds to disperse any large aggregates, and 100 μL of an aqueous solution of a fluorescent dye or enzyme was then added, and the mixture hand-shaken vigorously for 1 minute to facilitate water droplet formation. The volume fraction of aqueous phase ($\phi_w$) relative to oil was fixed at 0.033, and the amount of silica nanoparticles used was 0.2 mg per μL of the aqueous phase.

Transfer of the copolymer-functionalized colloidosomes from the oil phase into a continuous aqueous phase without loss of the compartmentalized microstructure was achieved as follows. Firstly, cross-linking the outer surface of the silica nanoparticle membrane was undertaken by addition of 0.27 mmol (40 μL) of oil-soluble TMOS to 3 mL of a pre-formed Pickering emulsion. The dispersion was gently rotated for 15 minutes in the dark using an Agar Scientific Rotator or stored in a fridge with occasional rotation for samples prepared with entrapped fluorescent dyes or enzymes, respectively. Secondly, functionalization of the silica cross-linked surface was undertaken by addition of 8 μL of the pH-responsive copolymer **1** (0.26 mM in methanol), followed by rotation either in the dark at room temperature (dye-containing colloidosomes) or in the fridge with occasional rotation (enzyme-containing colloidosomes) for 3 days. The copolymer-grafted colloidosomes were then transferred from the oil phase into a continuous aqueous phase by addition of 100 μL of acetone to 3 mL of the colloidosomes in oil; the unstirred mixture was then left at room temperature or in the fridge for 30 minutes, and another 100 μL of acetone added and the dispersion gently rotated, left for another 30 minutes, and then the transparent upper oil phase was discarded and the remaining lower phase gently re-dispersed in 1 mL of acetone and centrifuged at 4000 rpm for 30 s. The copolymer-coated colloidosomes were then re-dispersed in 1 mL of a mixture of acetone and aqueous buffer solution (1:1 v/v, pH = 7). The dispersion

was then centrifuged at 4000 rpm for 1 min and the clear upper solution was discarded. This was repeated with 1 mL of an aqueous buffer solution, and finally the droplets were re-suspended in 3 mL buffer solution at pH = 7.

**Imaging studies.** Optical and fluorescence microscopy images of the dye-entrapped colloidosomes dispersed in oil or in aqueous solutions at various pH values were recorded using a Leica DMI3000 B manual inverted fluorescence microscope at 10x or 20x magnification. Three band pass filters were used: excitation at 450-490 nm with an emission cut off at 510 nm (I3), excitation at 355-425 nm with an emission cut off at 455 nm (D), and excitation at 515-560 nm with an emission cut off at 580 nm (N2.1). Line intensity profiles on individual colloidosomes were processed from optical micrographs using Gwyddion software. Fluorescence images were collected at different pH values on over fifty individual colloidosomes and no qualitative difference in permeability behaviour was observed in each case. Calibration curves were determined by fluorescence spectroscopy (Jasco FP-6500) measurements on 0.1 mM bulk aqueous solutions of calcein, acriflavine hydrochloride or rhodamine 6G at pH values between 2 and 10. Excitation at 495 nm (calcein), 416 nm (acriflavine hydrochloride) or 526 nm (rhodamine 6G), and excitation and emission band widths of 3 nm and 1 nm were used, respectively.

**Release studies.** UV-vis spectroscopy was used to determine release profiles for cross-linked, copolymer-functionalized colloidosomes containing calcein or rhodamine 6G when transferred into a bulk water phase. Cross-linked, copolymer-functionalized colloidosomes were prepared in oil using an aqueous (pH = 7) solution of calcein (0.2 mM), acriflavine hydrochloride (0.2 mM) or rhodamine 6G (0.2 mM), and then transferred into 0.5 mL acetone as described above. The suspensions were centrifuged and the acetone removed, and the colloidosome dispersion then left for 30- 60 minutes in air to remove any residual acetone by evaporation. Buffered water (2 mL) at various pH values was then added and the concentration of the dye in the continuous aqueous phase measured with time. The time-dependent concentrations of released dye in the continuous phase were evaluated using UV-vis spectroscopy calibration curves determined at pH values of 2 (or 4), 7 and 9 (or 10) over a range of dye concentrations (Supplementary Figs S15 and 16). In each case, a finite dye concentration was observed at the first time point ($t_0$ = 30 min) due to the presence of broken colloidosomes in the dispersion originating from the transfer process. This was accounted for in the release profiles by plotting the effective concentration at time $t$, ($C'_t$), which was determined as $C'_t = (C_t - C_0)$ where $C_t$ and $C_0$ were the measured dye concentrations at $t$ and $t$ = 30 min.

**Uptake studies.** For uptake experiments, TMOS-cross-linked, copolymer functionalized water-in-oil colloidosomes were transferred into buffer at various pHs and washed twice with buffer. After centrifugation, the buffer was discarded and an aqueous solution of calcein or

acriflavine hydrochloride prepared at various buffered pH values was added to the colloidosome dispersion. Fluorescent images were then recorded within 2-3 hours. The recorded background intensity was susceptible to photo-bleaching during exposure to the light excitation source. As a consequence, uptake of the dyes into the colloidosomes often resulted in higher apparent fluorescence intensities compared with the background. This artefact could be minimised by recording images within 30 s of exposure to the light source.

**Influence of membrane permeability on enzymatic activity in inorganic protocells.** 100 μL of a 0.006U/μL solution of alkaline phosphatase (ALP) in Tris buffer (pH 7.2) was added to 3 mL of anhydrous dodecane containing 20 mg of partially hydrophobic silica nanoparticles, and the dispersion hand-shaken to produce a water-in-oil enzyme-containing Pickering emulsion. As described above, the external surface of the colloidosomes was cross-linked using TMOS, and functionalized with pH-responsive copolymer **1**, and then transferred into a water phase as intact enzyme-containing micro-compartments. 0.5 mL of glycine buffer (100 mM, with 1.0 mM magnesium chloride) at various pH values was added to 0.5 mL of the colloidosome dispersion (containing 0.1 U ALP inside the droplets). The dispersions were sedimented and the addition of buffer solutions repeated a few times to ensure that the required final pH was attained, and that no ALP molecules that may have originated from the disassembly of colloidosomes during transfer into water were present in the continuous phase. The final pH values were 8.4, 9.1 and 9.8. 10 μL of a 0.76 M aqueous solution of the phosphatase substrate, 4-nitrophenyl phosphate (*p*NPP, disodium salt hexahydrate) was then added to the continuous aqueous phase, and formation of the enzyme-mediated dephosphorylated product 4-nitrophenolate in the continuous aqueous phase at various pH values was monitored over time at 410 nm by UV-vis spectroscopy (Perkin Lambda II UV-VIS spectrometer). The reactions were maintained at 37 ºC using a PTP-6 Peltier temperature controller. Control experiments were run at the above pH values in bulk aqueous solutions of ALP in the absence or presence of copolymer-functionalized silica nanoparticles. The former gave calibration curves with a constant molar extinction constant of ($\varepsilon = 18300\ M^{-1}\ cm^{-1}$). The latter were prepared by mixing 20 mg of the partially hydrophobic silica nanoparticles with 3 mL of dodecane, followed by addition of 3 μL of water, and sonication for few minutes to disassemble the silica particle-stabilized droplets. 0.27 mmol (40 μL) of oil-soluble TMOS was then added to the oil phase followed by addition of 8 μL of the pH-responsive polymer **1** (0.26 mM in methanol) and stirring of the mixture at room temperature for 3 days. The copolymer-grafted silica nanoparticle aggregates were transferred to water by the same procedure used for the transfer of the colloidosomes. The copolymer and silica components had no effect on the enzymatic rates over the relevant pH range.

**References**


1. Stano, P., Carrara, P., Kuruma, Y., Souza, T & Luisi, P.L. Compartmentalized reactions as a case of soft-matter biotechnology: synthesis of proteins and nucleic acids inside lipid vesicles. *J. Mater. Chem.,* **21**, 18887-18902 (2011).
2. Pohorille, A. & Deamer, D. Artificial cells: prospects for biotechnology. *Trends in Biotech.,* **20**, 123-128 (2002).
3. Städler, B., *et al*. Polymer hydrogel capsules: en route toward synthetic cellular systems. *Nanoscale*, **1**, 68-73 (2009).
4. Szostak, J. W., Bartel, D. P. & Luisi, P. L. Synthesizing life. *Nature*, **409**, 387-390 (2001).
5. Mann, S. Systems of creation: the emergence of life from non-living matter. *Acc. Chem. Res.*, **45**, 2131-2141(2012).
6. Stano, P. & Luisi, P. L. Achievements and open questions in the self-reproduction of vesicles and synthetic minimal cells. *Chem. Commun*., **46**, 3639-3653 (2010).
7. Dzieciol, A. & Mann, S. Designs for life: protocell models in the laboratory. *Chem. Soc. Rev*., **41**, 79-85 (2012).
8. Walde, P. Building artificial cells and protocell models: experimental approaches with lipid vesicles. *Bioessays*, **32**, 296-303 (2010).
9. Koga, S., Williams, D. S., Perriman, A. W. & Mann, S. Peptide/nucleotide micro-droplets as a step towards a membrane-free protocell model. *Nature Chem.*, **3**, 720-724 (2011).
10. Williams, D. S., *et al.* Polymer/nucleotide droplets as bio-inspired functional micro-compartments. *Soft Matter*, **8**, 6004-6014 (2012).
11. Li, M., Green, D. C., Anderson, J. L. R., Binks, B. P. & Mann, S. *In vitro* gene expression and enzyme catalysis in bio-inorganic protocells. *Chem. Sci.*, **2**, 1739-1745 (2011).
12. Cooper, G. J. T., *et al.* Modular redox-active inorganic chemical cells: iCHELLs. *Angew. Chem. Int. Ed.,* **50***,* 10373-10376 (2011).
13. Subramaniam, A. B., Wan, J., Gopinath, A. & Stone, H. A. Semi-permeable vesicles composed of natural clay. *Soft Matter*, **7**, 2600-2612 (2011).
14. Dinsmore, A. D., *et al.* Colloidosomes: Selectively permeable capsules composed of colloidal particles. *Science*, **298**, 1006-1008 (2002).
15. Wu, C., Bai, S., Ansorge-Schumacher, M. B. & Wang, D. Nanoparticle cages for enzyme catalysis in organic media. *Adv. Mater.*, **23**, 5694-5699 (2011).
16. Boker, A., He, J., Emrick, T. & Russell, T. P. Self-assembly of nanoparticles at interfaces. *Soft Matter*, **3**, 1231-1248 (2007).
17. Wang, D. Y., Duan, H. W. & Mohwald, H. The water/oil interface: the emerging horizon for self-assembly of nanoparticles. *Soft Matter*, **1**, 412-416 (2005).

18. Shah, R. K., Kim, J.-W., & Weitz, D. A. Monodisperse stimuli-responsive colloidosomes by self-assembly of microgels in droplets. *Langmuir*, **26**, 1561-1565 (2010).
19. Hsu, M. F., *et al.* Self-assembled shells composed of colloidal particles: fabrication and characterization, *Langmuir*, **21**, 2963-2970 (2005).
20. Thompson, K. L. & Armes, S. P. From well-defined macromonomers to sterically-stabilized latexes to covalently cross-linkable colloidosomes: exerting control over multiple length scales. *Chem. Commun*., **46**, 5274-5276 (2010).
21. Subramaniam, A. B., Abkarian, M. & Stone, H. A. Controlled assembly of jammed colloidal shells on fluid droplets. *Nat. Mater*., **4**, 553-556 (2005).
22. Kim, J.-W., *et al.* Colloidal assembly route for responsive colloidosomes with tunable permeability. *Nano Lett*., **7**, 2876-2880 (2007).
23. Lee, D. & Weitz, D. A. Double emulsion-templated nanoparticle colloidosomes with selective permeability. *Adv. Mater*., **20**, 3498-3503 (2008).
24. Weaver, J. V. M. & Adams, D. J. Synthesis and application of pH-responsive branched copolymer nanoparticles (PRBNs): a comparison with pH-responsive shell cross-linked micelles. *Soft Matter*, **6**, 2575-2582 (2010).
25. Harbron, R. L., McDonald, T.O., Rannard, S. P., Findlay, P. H. & Weaver J. V. M. One-pot, single-component synthesis of functional emulsion-templated hybrid inorganic-organic polymer capsules. *Chem. Commun.,* **48**, 1592-1594 (2012).
26. Martin, W. & Russell, M. J. On the origins of cells: a hypothesis for the evolutionary transitions from abiotic geochemistry to chemoautotrophic prokaryotes, and from prokaryotyes to nucleated cells. *Phil. Trans. R. Soc. Lond. B.* **358**, 59-85 (2003).
27. Binks, B. P. & Murakami, R. Phase inversion of particle-stabilized materials from foams to dry water. *Nat. Mater*., **5**, 865-869 (2006).

**Acknowledgements**
We thank Parogle Technologies Ltd for a CASE funded studentship for R.L.H, and Anita Peacock (Centre for Materials Discovery, University of Liverpool) for running GPC samples. We thank EPSRC and the ERC (Advanced Grant scheme) for financial support.

**Author contributions**
M.L and S.M conceived the concept, S.M directed the research, M.L and R.L.H and J.V.M.W designed and performed the experiments and analysed the data, B.P.B contributed the surface-active nanoparticles and discussions on colloid science. All of the authors participated in writing the paper.

**Additional information**
The authors declare no competing financial interests. Supplementary information accompanies the paper at www.nature.com/naturechemistry. Correspondence and requests for materials should be addressed to M.L and S.M.

**Figure 1**. **Chemical construction of water-dispersible, aqueous inorganic micro-compartments with self-activated gated membrane permeability**. **a,** Scheme illustrating design and construction of functionalized colloidosomes prepared by TMOS-induced cross-linking and covalent grafting of a branched copolymer corona on the semi-permeable outer surface of a closely packed shell of silica nanoparticles. pH-induced changes in the net charge associated with cationic dimethylamino (blue) and anionic carboxylate (red) groups of the $TMSPMA_{23}/DMAEMA_{40}/MAA_{37}$-$EGDMA_8$-$DDT_{10}$ copolymer layer generates a gated response to the transfer of charged small molecules across the inorganic membrane. The structure of the branched copolymer is shown on the top right. **b,** Scheme showing the intersection of three closely packed silica nanoparticles located within the inorganic membrane; the associated chemical modifications and their effect on the structure and functionality of the inter-particle void space are shown.

**Figure 2. Optical micrographs of silica nanoparticle-stabilized aqueous micro-compartments. a,b,** Colloidosomes dispersed in oil before (**a**) and after (**b**) TMOS-mediated cross-linking and copolymer-functionalization of the inorganic membrane. **c**, After transfer of (**b**) into a bulk water phase. **d-f,** Structural properties of cross-linked, copolymer-functionalized colloidosomes; consecutive optical images showing deflation and elastic response of the inorganic membrane during air drying.

**Figure 3. Release properties of inorganic cell-like microstructures. a-d,** Calcein-containing TMOS-cross-linked colloidosomes: **a**, fluorescence microscopy image of an individual colloidosome dispersed in oil showing retention of the dye within the micro-compartment; **b,c,** fluorescence microscopy images of individual micro-compartments dispersed in water at pH 2.5 (**b**) and 10 (**c**) showing loss of fluorescence intensity attributed to pH-independent release of the dye. **d,** qualitative intensity line profiles for single colloidosomes shown in (**a**), (**b**) and (**c**) (black, red and green plots, respectively; *x* axis, position across colloidosome; *y* axis, relative intensity). **e-g,** Fluorescence images of individual calcein-containing cross-linked copolymer-functionalized colloidosomes prepared at an initial pH of 7 and dispersed in water at pH 4 (**e**), 7 (**f**) or 10 (**g**) showing progressive retention of the entrapped dye with increasing pH. **h,** Corresponding intensity profiles for single colloidosomes shown in (**e-g**) at pH 2 (black), 7 (pink) or 10 (blue). **i-k,** Fluorescence images of individual acriflavine hydrochloride-containing cross-linked copolymer-functionalized colloidosomes dispersed in water at pH 2 (**i**), 7 (**j**) or 10 (**k**) showing progressive leaching of the entrapped dye with increasing pH. **l,** Corresponding intensity profiles for single colloidosomes shown in (**i-k**) at pH 2 (black), 7 (pink) or 10 (blue). **m,n,** Plots showing concentration of dye molecules released into bulk aqueous solution for cross-linked copolymer-functionalized colloidosomes containing entrapped calcein at pH values of 4 (black circles), 7 (pink squares) or 10 (blue triangles) (**m**), or rhodamine 6G at pH values of 2 (black circles), 7 (pink squares) or 9 (blue trangles) (**n**) (see Methods for details). Scale bar for **a-c** and **e-k** = 100 μm. Fluorescence images were recorded 3-5 hours after transfer into a continuous aqueous phase.

**Figure 4. Uptake properties of cross-linked copolymer-functionalized colloidosomes**. Optical fluorescence images of (**a-c**) water-filled colloidosomes immersed in aqueous solutions of calcein at pH values of 10 (**a**), 7 (**b**) or 4 (**c**), or immersed in aqueous solutions of acriflavine hydrochloride at pH values of 10 (**d**), 7 (**e**) or 2 (**f**). Note the absence of dye uptake in (**a**) and (**f**). Scale bars = 200 μm.

**Figure 5. Enzyme-mediated dephosphorylation in inorganic protocells. a**, Plots showing time-dependent changes in 4-nitrophenolate concentrations in the continuous aqueous phase of a suspension of ALP-containing, copolymer-grafted cross-linked colloidosomes at pH values of 8.4 (black circles), 9.1 (red squares) and 9.8 (blue triangles); in each case initial rates are shown as dashed lines. **b,c,** Corresponding plots as in (**a**) but for cross-linked colloidosomes without a copolymer corona at pH values of 8.4 (black circles), 9.1 (red squares) and 9.8 (blue triangles) (**b**), or for ALP-mediated *p*NPP dephosphorylation in bulk aqueous solution at pH 8.4 (black), 9.1 (red) and 9.8 (blue) (**c**). **d**, Correlation rate curves for enzyme-mediated dephosphorylation against pH in cross-linked copolymer-modified colloidosomes (1), cross-linked colloidosomes (2), and in bulk aqueous solution (3).

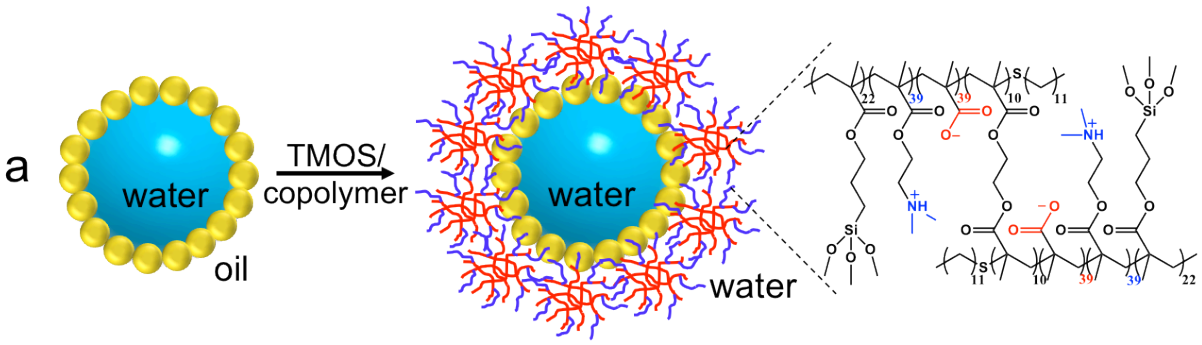
a
water
oil
TMOS/
copolymer
water
water

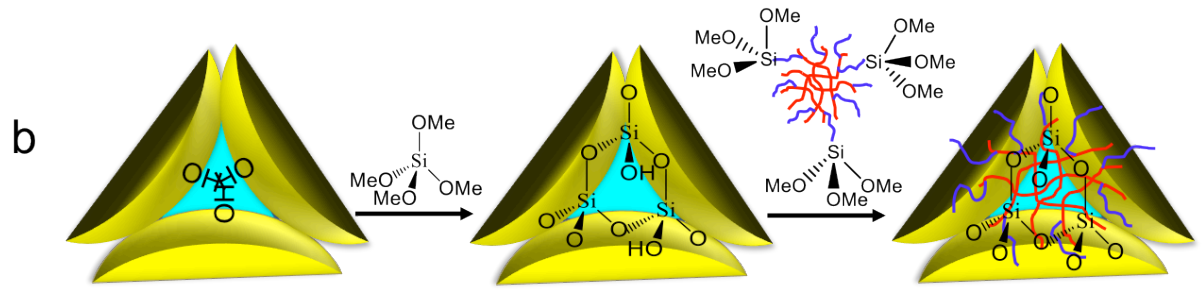
b
OMe
MeO
MeO
Si
OMe
HO
OH

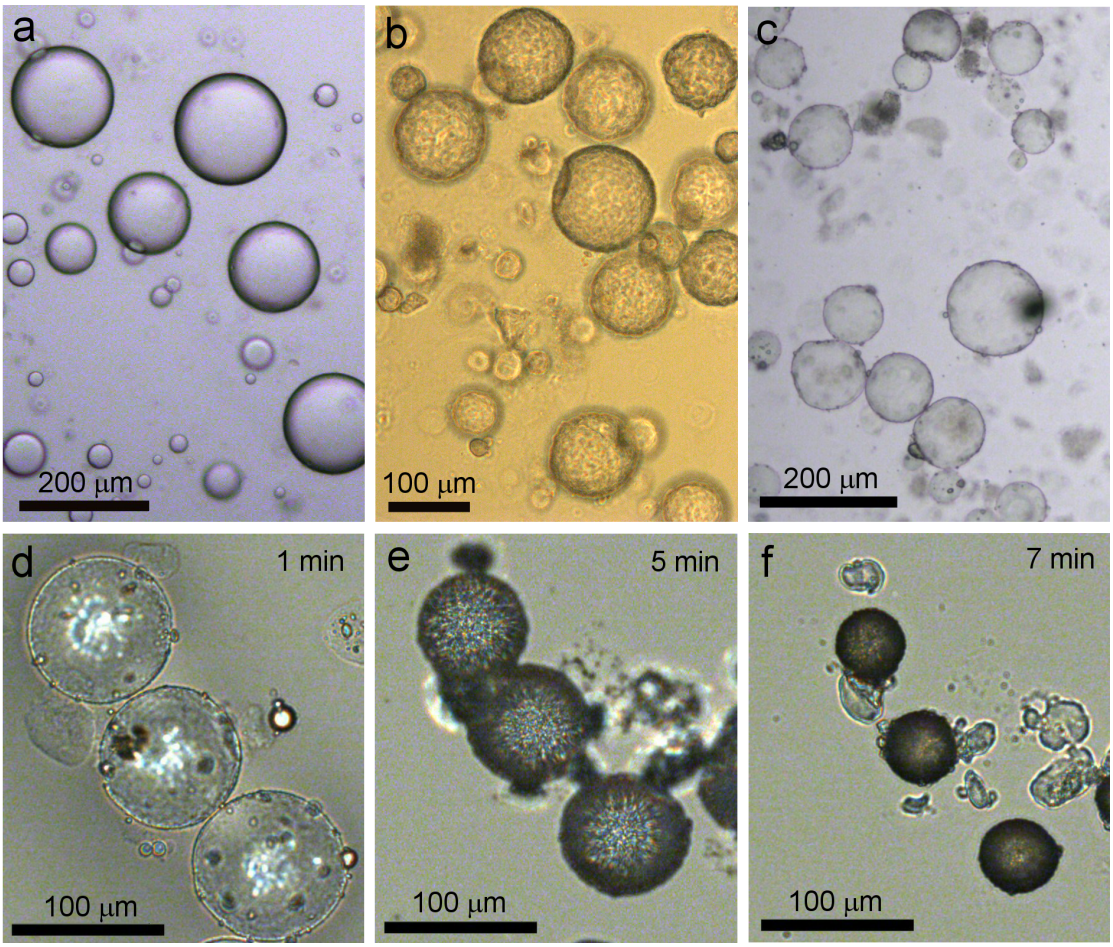
a
200 μm
b
100 μm
c
200 μm
d
1 min
100 μm
e
5 min
100 μm
f
7 min
100 μm

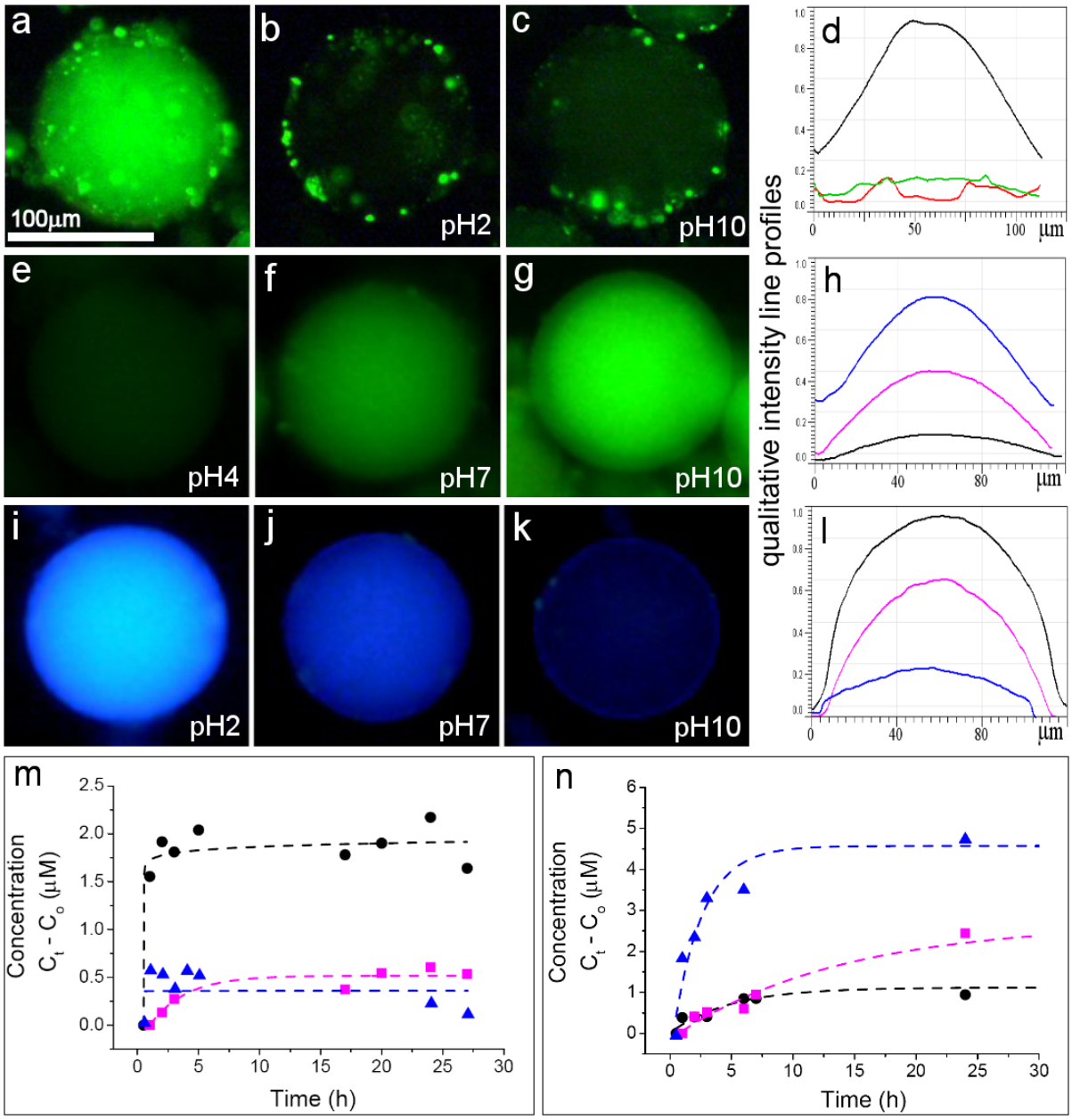
a
100μm
b
pH2
c
pH10
d
e
pH4
f
pH7
g
pH10
h
qualitative intensity line profiles
i
pH2
j
pH7
k
pH10
l
μm
m
Concentration
C_t - C_o (μM)
Time (h)
n
Concentration
C_t - C_o (μM)
Time (h)

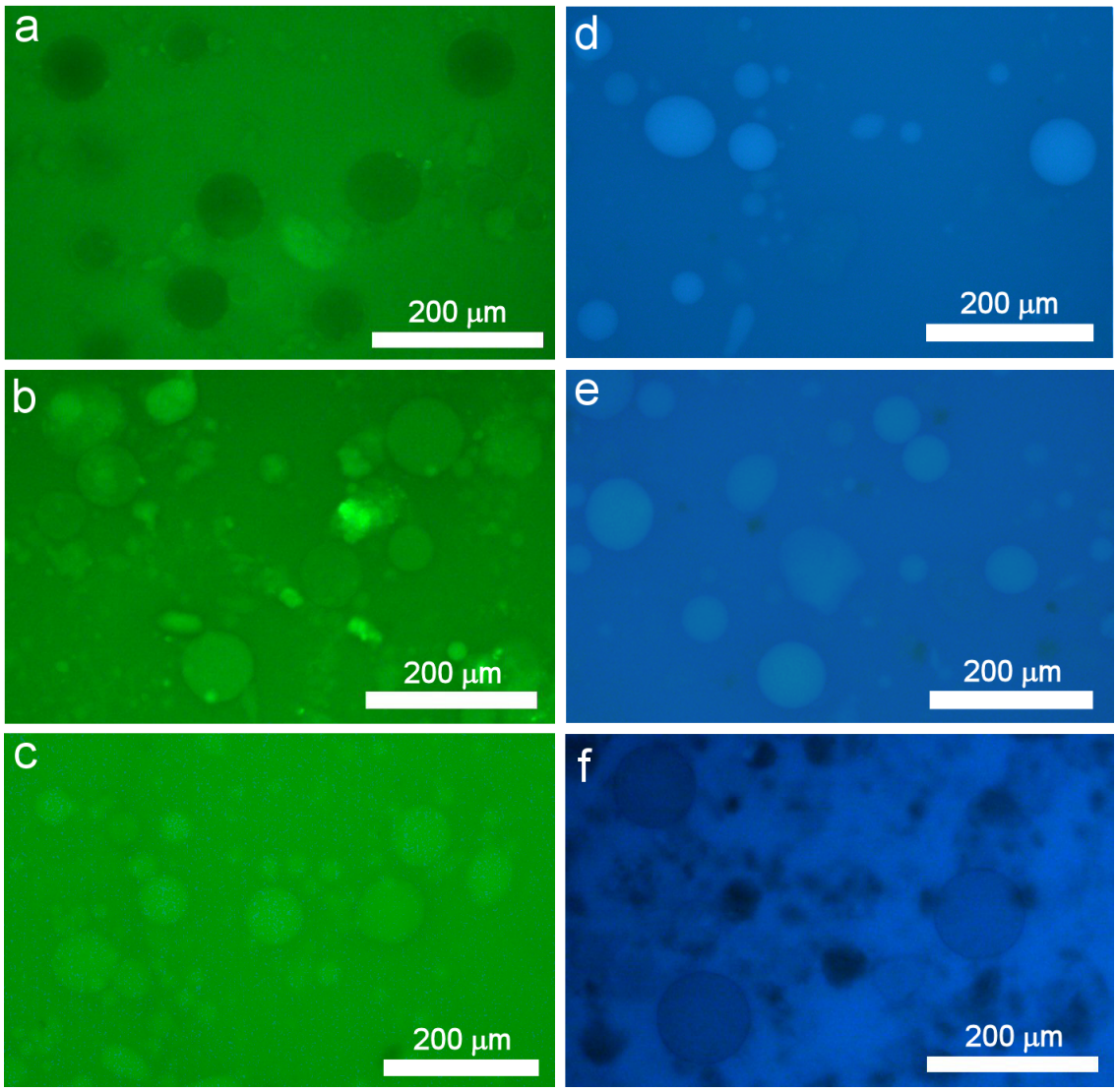
a
200 µm
d
200 µm
b
200 µm
e
200 µm
c
200 µm
f
200 µm

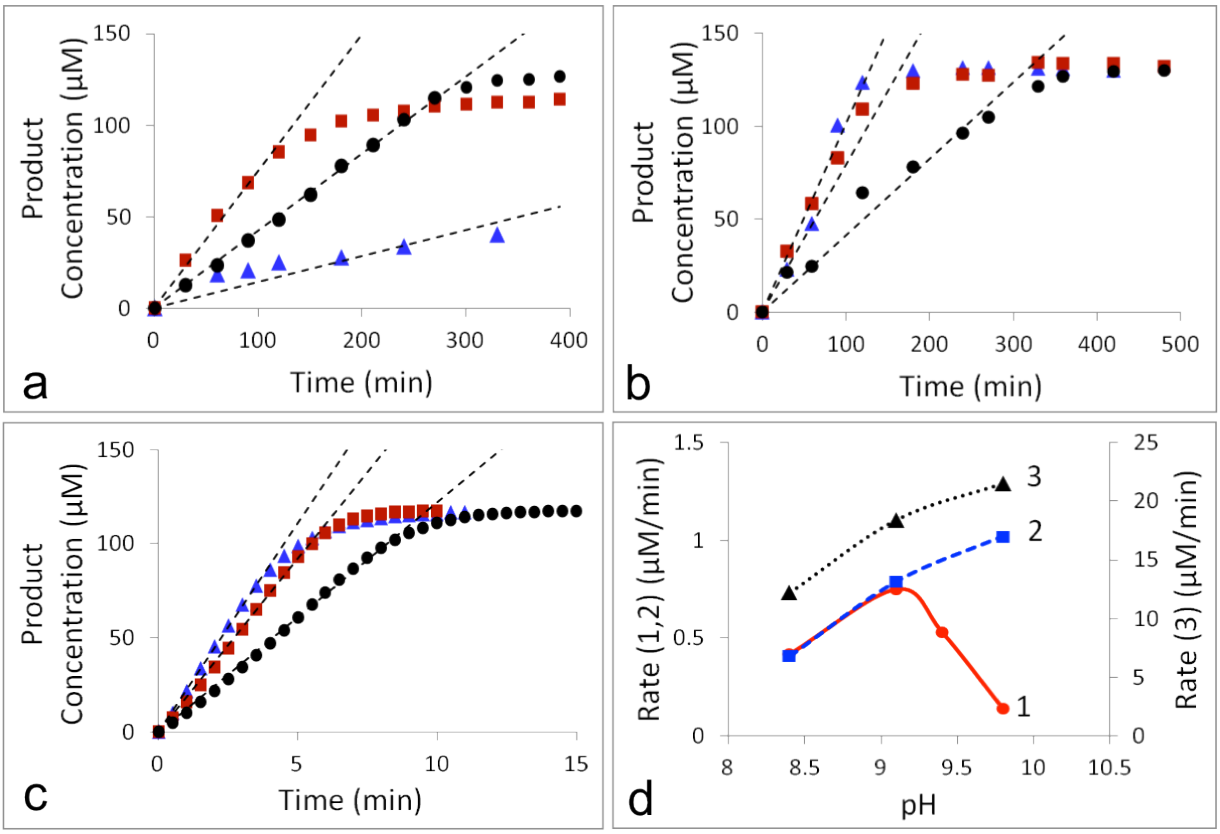
Product Concentration (µM)
Time (min)
a
b
c
d
Rate (1,2) (µM/min)
Rate (3) (µM/min)
pH
1
2
3